Pergamon

Scripta Materialia, Vol. 38, No. 4, pp. 537–542, 1998
Elsevier Science Ltd

1359-6462/98 $19.00 + .00

PII S1359-6462(97)00522-8

FATIGUE OF A Zr-Ti-Cu-Ni-Be BULK AMORPHOUS METAL: STRESS/LIFE AND CRACK-GROWTH BEHAVIOR

C.J. Gilbert, J.M. Lippmann and R.O. Ritchie
Department of Materials Science and Mineral Engineering, University of California, Berkeley, CA 94720-1760

(Received September 16, 1997)

Introduction

Bulk amorphous metals represent an exciting new class of structural materials, in part because of their near theoretical strength to modulus ratios and, in some cases, exceptional corrosion resistance (1). Traditionally, metallic glasses have been processed by rapid quenching ($>10^5$ K/s), thereby limiting mechanical property evaluation to very thin ($\sim$10–100 μm) ribbons or wires, e.g., (2–5). In the last few years, however, several families of multicomponent metallic alloys exhibiting excellent glass forming ability have been developed (6,7). Because resistance to the nucleation of equilibrium crystalline phases is high, conventional casting technologies and very low cooling rates ($<$10 K/s) are sufficient to produce an amorphous state. These alloys can thus be processed as *bulk* metallic glasses, permitting more extensive characterization of their mechanical properties.

In sharp contrast to oxide glasses, bulk metallic glasses can be surprisingly ductile. For example, recent experiments on a bulk $Zr_{41.2}Ti_{13.8}Cu_{12.5}Ni_{10}Be_{22.5}$ (at%) alloy have demonstrated that amorphous metals can exhibit fracture toughnesses as high as $\sim$55 MPa$\sqrt{m}$ (8,9), although mechanistically this result is not understood. Recent results also show fatigue-crack growth properties comparable to that of high-strength steels and aluminum alloys (8). However, corresponding stress/life (S/N) behavior on "smooth-bar," nominally crack-free specimens, which are traditionally used to assess total life and crack initiation characteristics, have to date not been investigated in bulk amorphous metals.

The question of S/N data is also important mechanistically since, although fatigue-crack *propagation* behavior appears to be similar to that seen in ductile crystalline metals, with clear evidence of striation formation (8), nothing is known about the susceptibility of bulk metallic glasses to crack *initiation*. In general, crack initiation in oxide glasses (and non phase-transforming ceramics) can only occur at pre-existing defects; natural (intrinsic) initiation of cracks cannot take place under cyclic loads. Conversely, crack initiation in crystalline metals can occur either at pre-existing flaws or intrinsically, e.g., through the development of persistent slip bands. Corresponding behavior in metallic glass alloys is unknown, although "slip" or shear band formation has been observed under monotonic loads, usually at high stresses or at low homologous temperatures (2,4).

Accordingly, the current study is focused on the S/N behavior of a bulk amorphous Zr-Ti-Cu-Ni-Be alloy, with the objective of examining the relationship between fatigue crack initiation and propagation in comparison to behavior in traditional crystalline alloys.

Experimental Procedures

As-received (7 mm thick, 40 × 40 mm) plates of the $Zr_{41.2}Ti_{13.8}Cu_{12.5}Ni_{10}Be_{22.5}$ (at%) fully amorphous alloy, were machined into 3 × 3 × 50 mm rectangular beams for S/N testing, and 7 mm thick, 38 mm wide compact-tension C(T) samples for crack-growth testing. Processing methods for this alloy are described in Ref. (6). The alloy displays a tensile yield strength of ~1900 MPa at which point catastrophic failure occurs (10).

Fatigue lifetimes, N_f, were measured over a range of cyclic stresses by cycling in four-point bending, with an inner span, S_1, and outer span, S_2, of 10.2 mm and 20.3 mm, respectively. Specimens, which had been previously polished to a ~1 μm surface finish, were cycled under load control at a frequency of 25 Hz (sinusoidal waveform) in a room air environment (25°C, ~45% relative humidity) on a servohydraulic mechanical test frame. The ratio of the minimum to maximum load, $R = \sigma_{min}/\sigma_{max}$, was maintained at 0.1 for all tests. Stresses were calculated at the tensile surface within the inner span from:

$$\sigma = \frac{3P(S_2 - S_1)}{2bh^2}, \tag{1}$$

where P is the applied load, b the specimen thickness, and h the specimen height. A total of 21 beams were tested at maximum stresses ranging from 100 MPa to 1800 MPa (just below the tensile failure stress), with multiple measurements made at each stress when possible. Tests were terminated in cases were failure had not occurred after 2×10^7 cycles (~9 days at 25 Hz). Fracture surfaces of selected beams were examined after failure via both optical and scanning electron microscopy (SEM) in order to discern the origin and mechanisms of failure. Stress/life data are presented in terms of the stress amplitude, $\sigma_a = \frac{1}{2}(\sigma_{max}\text{-}\sigma_{min})$, normalized by the tensile strength, σ_u, plotted as a function of the number of cycles to failure, N_f, where one cycle is defined as a full stress reversal.

Corresponding cyclic fatigue-crack growth rates, *da/dN*, were determined on fatigue precracked C(T) specimens under identical frequency, load ratio and environmental conditions. Test procedures were in general accordance with ASTM standard E647. Fatigue thresholds, ΔK_{TH}, below which crack growth is considered to be dormant, were operationally defined as the applied stress-intensity range, ΔK, below which $da/dN < 10^{-10}$ m/cycle. Thresholds were approached using a variable-ΔK/constant-R load-shedding scheme on a computer-controlled servohydraulic test frame. Crack lengths were continuously monitored using unloading elastic compliance measurements with a 350 Ω strain gauge attached to the back face of the specimen. A preliminary assessment of crack propagation in this alloy was reported previously in Ref. (8).

Results and Discussion

Crack-Growth Behavior

As reported previously (8), stable crack propagation is observed in the amorphous $Zr_{41.2}Ti_{13.8}Cu_{12.5}Ni_{10}Be_{22.5}$ alloy under cyclic loading. More extensive results for a number of specimens are shown in Fig. 1 in the form of growth rates, *da/dN*, plotted as a function of the applied stress-intensity range, ΔK, and are compared with behavior in a high strength steel (300-M, quenched and 200°C-tempered Si-modified 4340) (11) and an age-hardened aluminum alloy (2090-T81) (12). It is apparent that cyclic-crack growth rates in the metallic glass are comparable to those observed in traditional polycrystalline metallic alloys. Indeed, when regression fit to a simple Paris power-law relationship, $da/dN \propto \Delta K^m$ (13), the exponent m in the mid-range of growth rates (~10^{-10} to 10^{-7} m/cycle) lies in the range $m \sim 2$–4, typical of ductile metals in this regime. Moreover, in terms of a

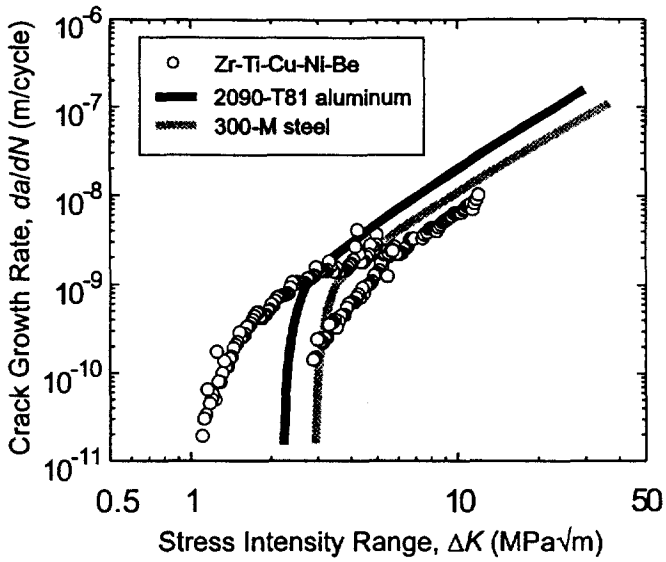

Figure 1. Fatigue-crack growth rates, *da/dN*, are plotted as a function of the stress-intensity range, ΔK, for the bulk amorphous alloy. Data include several specimens, and are compared to high-strength 300-M steel ($\sigma_u \sim 2300$ MPa) and 2090-T81 ($\sigma_u \sim 589$ MPa) aluminum alloys.

simple crack-tip opening displacement (CTOD) model for crack growth (14), the crack-growth increment is ~0.01 of the computed ΔCTOD per cycle (8). Such behavior is in marked contrast to the fatigue properties of oxide glasses (15) and other ceramics (16,17), where the exponent m typically ranges from as high as 15 to over 50. With respect to fatigue thresholds, values of ΔK_{TH} in the metallic glass ranged from ~1 to 3 MPa$\sqrt{m}$, which is again comparable to many higher strength steel and aluminum alloys. However, whereas specimen-to-specimen variation in $da/dN(\Delta K)$ data was small in the mid-growth rate regime, a high degree of scatter was found at near-threshold levels (possibly due to residual stresses).

While the mechanisms for fatigue-crack propagation in amorphous alloys are unclear, they are most likely similar to those in crystalline metals as ductile striations have been detected on fatigue fracture surfaces in this bulk alloy (8), as well as in previous studies of fatigue in thin amorphous ribbons (18–20). Models for striation formation require some degree of irreversible slip at the crack tip which acts to alternately blunt and re-sharpen the crack during the loading and unloading cycle. Although dislocation activity is clearly not present (at least not as it is understood in crystalline metals), tensile experiments have indicated that highly localized shear deformation precedes failure in this and many other amorphous metals (10,21), and it is presumed that such localized shear provides a mechanism for crack-tip blunting.

Stress/Life Behavior

The normalized stress amplitude, σ_α/σ_u, is plotted as a function of cycles to failure, N_f, for the $Zr_{41.2}Ti_{13.8}Cu_{12.5}Ni_{10}Be_{22.5}$ alloy in Fig. 2. Results are again compared with that for 300-M high strength steel (22) and the 2090-T81 aluminum-lithium alloy (23). It is clear from Fig. 2 that despite the similarity in crack-growth properties of bulk amorphous metals to polycrystalline metals (Fig. 1), the S/N properties are very different. Not only are fatigue lifetimes significantly shorter in the metallic

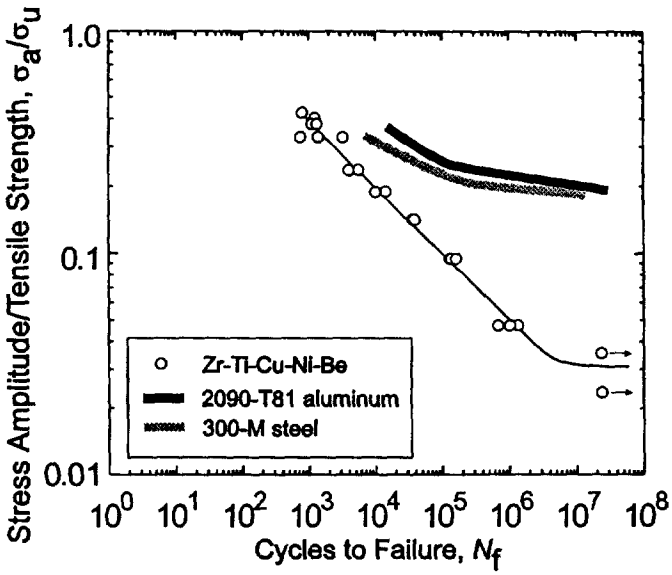

Figure 2. Stress/life data are presented in terms of the stress amplitude, $\sigma_a = \frac{1}{2}(\sigma_{max}-\sigma_{min})$, normalized by the tensile strength, σ_u, plotted as a function of the number of cycles to failure, N_f, for both the bulk metallic glass and high-strength steel and aluminum alloys.

glass (at a given value of σ_α/σ_u), but lifetimes exhibit a much lower dependence on the stress amplitude. For example, by fitting the S/N data to the simple (Basquin) equation $(\sigma_\alpha)^n N_f$ = constant, fatigue lives in the metallic glass are proportional to $(\sigma_\alpha)^{-3.4}$, compared to the more common result of $(\sigma_\alpha)^{-10}$ in steel and aluminum. Moreover, whereas steel and aluminum alloys generally display a fatigue limit or 10^7-cycle endurance strength at values of σ_α/σ_u between 0.3 and 0.5 (for $R = 0.1$), no such fatigue limit can be detected in the metallic glass until σ_α/σ_u drops below ~0.04. These results are consistent with previous studies on rapidly-quenched thin ribbons of metallic glass which also indicate a low dependence of fatigue life on the applied stress amplitude (18,19).

Careful optical examination of fatigue fracture surfaces indicates that cracking originates from a corner of the beam at the tensile face of the specimen, with the extent of stable fatigue-crack propagation increasing with life. At long lives, where $N_f > 10^6$ cycles, the fatigue fracture surface contains large regions which display a mirror-like appearance with no detectable evidence of topographical features. Indeed, previous studies on crack propagation revealed that the roughness of the fatigue surfaces in this alloy progressively diminishes with decreasing growth rates, leading to a mirror-like morphology at near-threshold levels (i.e., at $da/dN \sim 10^{-10}$ m/cycle) (8). The origin of such behavior is unknown but almost certainly involves extensive sliding crack-surface interference between the mating crack surfaces. Detailed SEM analysis of the fracture surfaces indicate a very distinct transition from stable fatigue-crack propagation to overload fracture. For example, the montage in Fig. 3 (representing an area ~70 × 110 μm) indicates striation-type growth in the fatigue region on the left, followed by an abrupt change to a vein morphology characteristic of overload fracture in metallic glasses (5).

The results in Figs. 1 and 2 present an interesting contrast between crystalline and amorphous metals. Whereas the crack-propagation properties are similar in the two classes of materials (with respect to the presence of fatigue striations (8) and the dependence of growth rates on ΔK), the S/N behavior is markedly different. Total life is far less dependent upon the applied stress amplitude and the fatigue

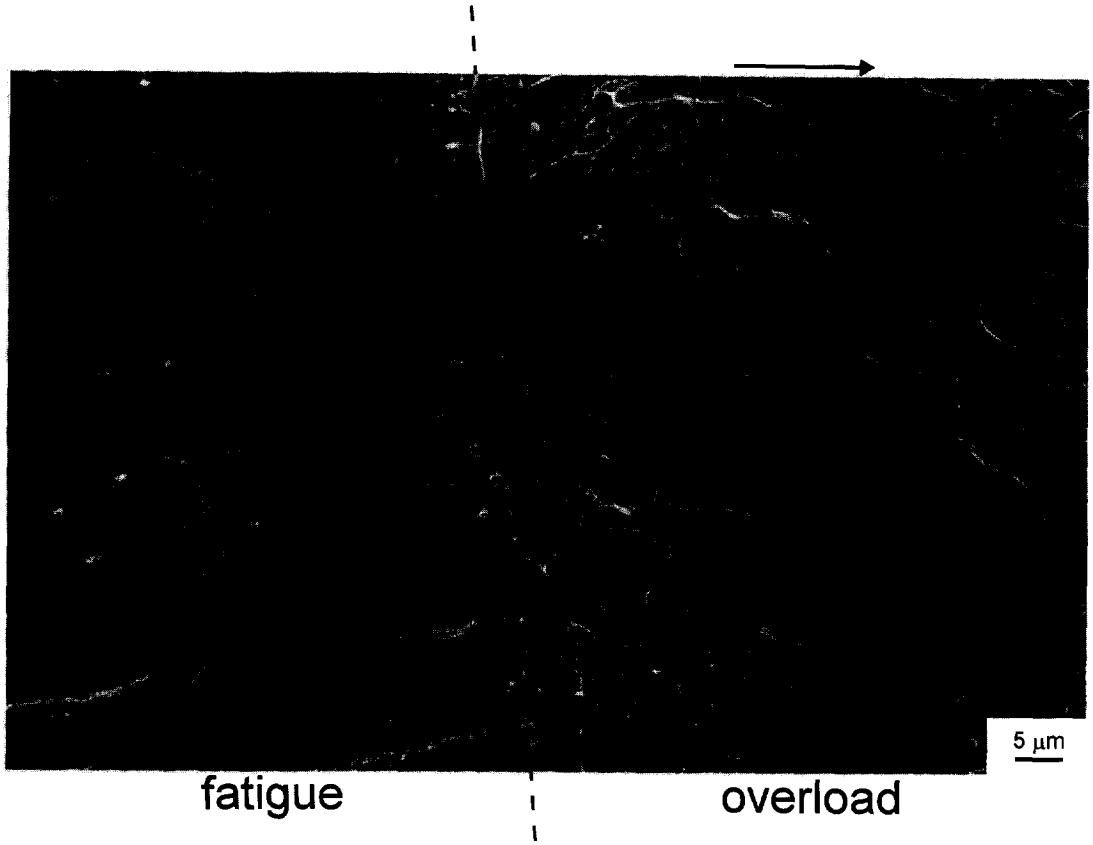

Figure 3. Scanning electron micrograph of the boundary between fatigue and overload fracture on the surface of a beam broken under cyclic loads ($N_f \sim 1.3 \times 10^6$ cycles, $\sigma_\alpha = 90$ MPa). The applied stress intensity range varied from ~40 to 50 MPa$\sqrt{m}$ in the fatigue region (on the left of this micrograph). The arrow represents the nominal direction of crack propagation, and the dotted line marks the boundary between fatigue and overload fracture.

limit is smaller by an order of magnitude. This implies that mechanistically the fatigue properties of crystalline and amorphous metals differ significantly with respect to crack initiation, or more precisely in the nucleation of crack growth. This may be associated with the easier natural initiation of a fatigue crack, e.g., via "slip-band" formation (10), although nothing is known about the initiation mechanisms in these materials at this time. However, since the fatigue limit can be equated with the critical stress for crack initiation or more generally for an initiated (small) crack to "overcome" some microstructural barrier (e.g., a grain boundary) (24), we may presume that the markedly lower fatigue limits in the amorphous alloys may be associated with a lack of microstructure which would normally provide local arrest points.

Conclusions

Based on an experimental study of the cyclic fatigue behavior of a bulk metallic glass alloy, $Zr_{41.2}Ti_{13.8}Cu_{12.5}Ni_{10}Be_{22.5}$ (at%), involving both crack propagation (using precracked C(T) speci-

mens) and stress-life (S/N) (using nominally crack-free, unnotched beams) studies, the following conclusions can be made:

1. Crack-propagation behavior in the metallic glass was found to be similar to that observed in traditional ductile crystalline alloys (e.g., high-strength steels and aluminum alloys), both in terms the dependence of growth rates on the applied stress-intensity range and in the presence of ductile striations on fatigue fracture surfaces.
2. Conversely, the stress-life behavior of the metallic glass (at $R \sim 0$) was very different from that observed in the crystalline alloys. Fatigue lifetimes were much shorter in the amorphous alloy and exhibited a far lower dependence on the applied stress range; moreover, no evidence of a fatigue limit could be detected until stress amplitudes dropped below $\sim 1/25$ of the tensile strength.
3. Given the similarity in crack-growth behavior but the very different stress/life properties, the prime distinction in the cyclic fatigue behavior of ductile crystalline and bulk amorphous metals appears to be that the ease of crack initiation in the metallic glass is far less sensitive to the applied stress.

Acknowledgments

This work was supported by the U.S. Air Force Office of Scientific Research, under Grant No. F49620-1-0365. Thanks are also due to Dr. A. Peker and Dr. M. Tenhover of Amorphous Technologies International, Corporation for their support and for supplying the material, and to Prof. W. L. Johnson for helpful discussions.

References

1. W. L. Johnson, Current Opinion in Sold State and Materials Science, 1, 383 (1996).
2. J. J. Gilman, J. Appl. Phys. 46, 1625 (1975).
3. T. Masumoto and R. Maddin, Acta Metall. 19, 725 (1971).
4. H. J. Leamy, H. S. Chen, and T. T. Wang, Metall. Trans. 3, 699 (1972).
5. C. A. Pampillo and A. C. Reimschuessel, J. Mat. Sci. 9, 718 (1974).
6. A. Peker and W. L. Johnson, Appl. Phys. Lett. 63, 2342 (1993).
7. A. Inoue, T. Zhang, and A. Takeuchi, Appl. Phys. Lett. 71, 464 (1997).
8. C. J. Gilbert, R. O. Ritchie, and W. L. Johnson, Appl. Phys. Lett. 71, 476 (1997).
9. R. D. Conner, A. J. Rosakis, W. L. Johnson, and D. M. Owen, Scripta Mat., submitted March 1997.
10. H. A. Bruck, T. Christman, A. J. Rosakis, and W. L. Johnson, Scripta Metall. Mat. 30, 429 (1994).
11. R. O. Ritchie, J. Eng. Mat. Tech. Trans. ASME Series H. 99, 195 (1977).
12. K. T. Venkateswara Rao, W. Yu, and R. O. Ritchie, Metall. Trans. A. 9, 549 (1988).
13. P. C. Paris and F. Erdogan, J. Basic Eng. 85, 528 (1963).
14. F. A. McClintock, Boeing Technical Report, 1967, cited in R. M. N. Pelloux, Trans. ASM, 62, 281 (1969).
15. S. J. Dill, S. J. Bennison, and R. H. Dauskardt, J. Am. Ceram. Soc. 80, 773 (1997).
16. R. O. Ritchie and R. H. Dauskardt, J. Ceram. Soc. Japn. 99, 1047 (1991).
17. C. J. Gilbert, R. H. Dauskardt, R. W. Steinbrech, R. N. Petrany, and R. O. Ritchie, J. Mat. Sci. 30, 643 (1995).
18. T. Ogura, T. Masumoto, and K. Fukushima, Scripta Metall. 9, 109 (1975).
19. L. A. Davis, J. Mat. Sci. 11, 711 (1976).
20. L. A. Davis, J. Mat. Sci. 10, 1557 (1975).
21. C. A. Pampillo and D. E. Polk, Acta Metall. 22, 741 (1974).
22. W. F. Brown, Jr., Aerospace Structural Metals Handbook, Code 1224, Metals and Ceramics Information Center, 1–30 (1989).
23. K. T. Venkateswara Rao and R. O. Ritchie, Int. Mat. Rev. 37, 153 (1992).
24. K. J. Miller, Fat. Fract. Eng. Matls. Struct. 10, 93 (1987).